



Chronostratigraphy of sediment cores from Lake Selina, southeastern Australia: Radiocarbon, optically stimulated luminescence, paleomagnetism, authigenic beryllium isotopes and elemental data

Agathe Lisé-Pronovost, Michael-Shawn Fletcher, Quentin Simon, Zenobia Jacobs, Patricia S Gadd, Andy I.R. Herries, Yusuke Yokoyama, Aster Team

► To cite this version:

Agathe Lisé-Pronovost, Michael-Shawn Fletcher, Quentin Simon, Zenobia Jacobs, Patricia S Gadd, et al.. Chronostratigraphy of sediment cores from Lake Selina, southeastern Australia: Radiocarbon, optically stimulated luminescence, paleomagnetism, authigenic beryllium isotopes and elemental data. Data in Brief, 2022, 42, pp.108144. 10.1016/j.dib.2022.108144 . hal-03937540

HAL Id: hal-03937540

<https://hal.inrae.fr/hal-03937540>

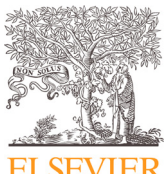
Submitted on 13 Jan 2023

HAL is a multi-disciplinary open access archive for the deposit and dissemination of scientific research documents, whether they are published or not. The documents may come from teaching and research institutions in France or abroad, or from public or private research centers.

L'archive ouverte pluridisciplinaire **HAL**, est destinée au dépôt et à la diffusion de documents scientifiques de niveau recherche, publiés ou non, émanant des établissements d'enseignement et de recherche français ou étrangers, des laboratoires publics ou privés.



Distributed under a Creative Commons Attribution - NonCommercial - NoDerivatives 4.0 International License



Data Article

Chronostratigraphy of sediment cores from Lake Selina, southeastern Australia: Radiocarbon, optically stimulated luminescence, paleomagnetism, authigenic beryllium isotopes and elemental data

Agathe Lisé-Pronovost^{a,b,*}, Michael-Shawn Fletcher^a, Quentin Simon^c, Zenobia Jacobs^d, Patricia S. Gadd^e, Andy I.R. Herries^b, Yusuke Yokoyama^f, Aster team^{c,1}

^a School of Geography, Earth and Atmospheric Sciences, University of Melbourne, Carlton, VIC 3053, Australia

^b Department of Archaeology and History, The Australian Archaeomagnetism Laboratory, Palaeoscience Labs, La Trobe University, Melbourne Campus, Bundoora, VIC 3086, Australia

^c CEREGE UM34, Aix Marseille University, CNRS, IRD, INRAE, Coll France, Aix en Provence, 13545, France

^d Australian Research Council Centre of Excellence for Australian Biodiversity and Heritage and School of Earth, Atmospheric and Life Sciences, University of Wollongong, Wollongong, NSW 2522, Australia

^e Australian Nuclear Science and Technology Organisation (ANSTO), New Illawarra Road, Lucas Heights 2234, Australia

^f Department of Earth and Planetary Sciences, Graduate School of Science, University of Tokyo, Chiba 277-8564, Japan

ARTICLE INFO

Article history:

Received 23 November 2021

Revised 29 March 2022

Accepted 30 March 2022

Available online 8 April 2022

ABSTRACT

This Data in Brief paper comprises dataset obtained for sediment cores collected from Lake Selina, located in the West Coast Range of Tasmania, Australia. Datasets include radiocarbon and optically stimulated luminescence age estimates, elemental composition, beryllium isotopes, magnetic properties and the paleomagnetic record measured on the cores assigned as TAS1402 (Location: Tasmania,

* Corresponding author at: School of Geography, Earth and Atmospheric Sciences, University of Melbourne, Carlton, VIC 3053, Australia.

E-mail address: agathe.lise@unimelb.edu.au (A. Lisé-Pronovost).

Social media: @Agathelp (A. Lisé-Pronovost)

¹ Georges Aumaître, Didier L. Bourlès†, Karim Keddadouche.



Keywords:

Paleomagnetism
 Optically stimulated luminescence
 Radiocarbon
 Authigenic $^{10}\text{Be}/^{9}\text{Be}$ ratio
 Lake sediments
 Australia
 Pleistocene
 Laschamp geomagnetic excursion

Year: 2014, Site number: 02). The multi-proxy dataset was used to develop a chronostratigraphy for the 5.5 m and 270,000 year old record. See Lisé-Pronovost et al. (2021) (10.1016/j.quageo.2021.101152) for interpretation and discussion. The data presented in this study serve as an archive for future studies focusing on Earth system dynamics and the timeline and linkages of environmental changes across Tasmania, the Southern Hemisphere and at a global scale.

© 2022 The Author(s). Published by Elsevier Inc.

This is an open access article under the CC BY-NC-ND license (<http://creativecommons.org/licenses/by-nc-nd/4.0/>)

Specifications Table

Subject	Earth and Planetary Sciences (General)
Specific subject area	Chronostratigraphy, paleoenvironment and paleomagnetism of Pleistocene lake sediment (5.5 m, 270 ka) from southeast Australia
Type of data	Table
How data were acquired	<p>Paleomagnetism and magnetic properties: Magnetic remanence measurements were performed using a 2G Enterprises Cryogenic magnetometer and pulse magnetiser. Principal component analysis of the magnetic remanence data was performed with the Puffinplot software [1].</p> <p>Hysteresis properties, isothermal remanent magnetisation (IRM) acquisition curves and first-order reversal curves were measured using a Princeton Measurements Corporation Vibrating Sample Magnetometer (VSM). IRM acquisition curves were analysed with the MAX Unmix software [2]. First-order reversal curves were processed with FORCinel software [3] with VARIFORC smoothing [4]. Low temperature analyses were performed with a Quantum Design Magnetic Properties Measurement System (MPMS). Room temperature and high temperature magnetic susceptibility measurements were performed with a AGICO Kappabridge MK2.</p> <p>Elemental data: Elemental composition was measured with an Itrax X-ray fluorescence (XRF) core scanner.</p> <p>Beryllium isotopes: Beryllium-10 (^{10}Be) cosmogenic nuclide concentrations were measured using an Accelerator Mass Spectrometer (AMS) HVE 4150. Beryllium-9 (^{9}Be) stable isotope analyses were performed using a graphite-furnace atomic absorption spectrophotometer (AAS) with a double beam correction (Thermo Scientific ICE 3400).</p> <p>Radiocarbon: Radiocarbon dating was conducted using an Accelerator Mass Spectrometer (AMS) National Electrostatics Corporation (NEC) 1.5 SDH Compact Pelletron 500kV (DirectAMS Radiocarbon Dating Service laboratory).</p> <p>Optically stimulated luminescence (OSL): All OSL measurements were made on a Risø TL-DA-20 luminescence reader [5]. Beta dose rate measurements was conducted on a Risø GM-25-5 beta counter [6]. Gamma dose rates were estimated from uranium and thorium concentrations determined by inductively coupled plasma mass spectrometry (ICP-MS) and inductively coupled plasma optical emission spectroscopy (ICP-OES) conducted at Intertek Genalysis, based in Perth, Western Australia. Analysis of the luminescence data, including curve fitting and error calculations, was conducted in Analyst software version 4.57 [7].</p>
Data format	Raw Analyzed

(continued on next page)

Parameters for data collection	All data was acquired from sediments retrieved from Lake Selina. Coring was completed from a floating platform rigged on two inflatable rafts. Sediment cores were collected in aluminium core liners and sealed with plastic caps and tape, then transported to The University of Melbourne and stored in a cold room. The aluminium core liners were split lengthwise using a GEOTEK core splitter. Sampling for OSL dating was done under red light after first removing those outer light-exposed portions of the core at the point of sampling.
Description of data collection	Three cores labelled TAS1402 were recovered from the approximate lake centre including a short gravity core LA (84 cm) and two Nesje [8] cores N1 (sections A, B, C; 394 cm) and N2 (sections A, B, C, D; 497 cm). X-ray fluorescence core scanning data was acquired on split half cores. The other split half cores were sampled for radiocarbon dating (29x bulk sediment 0.5 cm depth), OSL dating (23x sediment 3–7 cm depth), paleomagnetism (287 standard 8 cm ³ cube samples), magnetic properties (24 × 1 g dry sediment), and beryllium isotopes (45 × 1 g dry sediment).
Data source location	Lake Selina, Tasmania, Australia (41°52'41"S, 145°36'34"E)
Data accessibility	Repository name: PANGAEA Data identification number: 10.1594/PANGAEA.931786 Direct URL to data: protect-au.mimecast.com/s/4URHCxnMJ5s1zvRVPT8eQkl?domain=doi.pangaea.de
Related research article	Lisé-Pronovost, Agathe; Fletcher, Michael-Shawn; Simon, Quentin; Jacobs, Zenobia; Gadd, Patricia S; Heslop, David; Herries, Andy IR; Yokoyama, Yusuke (2021): Chronostratigraphy of a 270-ka sediment record from Lake Selina, Tasmania: Combining radiometric, geomagnetic and climatic dating. PANGAEA, 10.1594/PANGAEA.931786 Lisé-Pronovost, A., Fletcher, M.S., Simon, Q., Jacobs, Z., Gadd, P., Heslop, D., Herries, A.I.R., Yokoyama, Y., 2021. Chronostratigraphy of a 270-ka sediment record from Lake Selina, Tasmania: combining radiometric, geomagnetic, and climatic dating. <i>Quaternary Geochronology</i> 62, 101152. 10.1016/j.quageo.2021.101152

Value of the Data

- This multidisciplinary dataset provides information about the composition of the sediment in the TAS1402 cores from Lake Selina, Tasmania, their estimated ages, accumulation rates, and paleomagnetic record, spanning the last 270,000 years and several glacial and interglacial climates.
- The data can be used to compare the nature and timing of paleoclimate changes and events from Tasmania, the broader region and the world. Paleoclimate proxies of interest include the Southern Hemisphere westerly winds, atmospheric temperature and precipitation.
- The data and stratigraphy can be used to constrain the chronology of other cores extracted from Lake Selina and of other sites.
- The paleomagnetic data, including the sedimentary magnetic remanence and authigenic beryllium isotope ratios, can be used for regional to global paleomagnetic investigations and modelling. This dataset provides information on geomagnetic variations in a region that is currently poorly documented.

1. Data Description

Data are reported in table format as Excel sheets.

Dataset 1: Age_models_TAS1402

This dataset includes three tables. The first table contains the radiocarbon age estimates (including the sample name, depth, error on depth, radiocarbon age and error, and calibrated age and error). The second table contains the optically-stimulated luminescence (OSL) age estimates

(including the associated equivalent dose (D_e) and environmental dose rate information). The third table contains the three age-depth models (Radiometric, Match-Climate, Match-Dipole) discussed by Lise-Pronovost et al. [9].

Dataset 2: Be_data

This dataset is a table of the beryllium isotopes (^{10}Be , ^9Be) results and calculated $^{10}\text{Be}/^9\text{Be}$ ratio used as a geomagnetic intensity proxy. The data comprises the measured $^{10}\text{Be}/^9\text{Be}$ ratios from accelerator mass spectroscopy (AMS) measurements, decay-corrected ^{10}Be concentrations calculated from the AMS $^{10}\text{Be}/^9\text{Be}$ ratio, ^9Be concentrations determined from repeated absorbance measurements (standard-addition method), and the authigenic $^{10}\text{Be}/^9\text{Be}$ ratio.

Dataset 3: Pmag_data_Fig9

This dataset contains tables of the paleomagnetic data along the reference composite depth LAN2 presented in Fig. 9 of [9]. The first table includes the raw paleomagnetic data and principal component analysis results for all samples performed with Puffin Plot software. The second table includes the same data only for the selected samples that have passed the selection criteria. The third table includes the four discussed relative paleointensity proxies. They are the natural remanent magnetisation normalized by the anhysteretic remanent magnetisation after alternating demagnetisation at 20 mT (NRM20/ARM20), the natural remanent magnetisation normalized by the isothermal remanent magnetisation after alternating demagnetisation at 20 mT (NRM20/IRM20), the natural remanent magnetisation normalized by the anhysteretic remanent magnetisation for the portion of remanence between 60 and 10 mT (N/A(10-60)), and the natural remanent magnetisation normalized by the isothermal remanent magnetisation for the portion of remanence between 60 and 10 mT (N/I(10-60)).

Dataset 4: Pmag_data_Figs10_and_13

This dataset contains three tables of the paleomagnetic data presented in Figs. 10 and 13 of [9]. The first table includes the paleomagnetic inclination and declination along the reference composite depth LAN2 and the three age models (Radiometric, Match-Climate, Match-Dipole). The second table includes the raw data and selected relative paleointensity proxy (select RPI) along the reference composite depth LAN2 and the three age models (Radiometric, Match-Climate, Match-Dipole). The third table includes the beryllium isotopes ratio and uncertainties used as a geomagnetic field intensity proxy (select Beratio) along the reference composite depth LAN2 and the three age models (Radiometric, Match-Climate, Match-Dipole).

Dataset 5: Rock_magnetic_data

This dataset includes tables of magnetic properties measured on paleomagnetic cubes, including the low field magnetic susceptibility (kLF), the natural remanent magnetisation (NRM), the anhysteretic remanent magnetisation (ARM), the 1T isothermal remanent magnetisation (IRM_{1T}), the susceptibility of the ARM normalised by the IRM_{1T} (kARM/IRM_{1T}), the median destructive field of the ARM (MDF_{ARM}), the s-ratio defined as the isothermal remanent magnetisation at 0.3T in the opposite direction normalised by the IRM_{1T} (IRM_{0.3T}/IRM_{1T}) and the HIRM (defined as IRM_{1T} + IRM_{-0.3T})/2), as well as measured on discrete samples, including the remanence ratio (saturation remanence (Mr)/saturation magnetisation (Ms)). The samples of core N1 are assigned both their original depth in core N1 and their equivalent sample depth in the reference composite depth LAN2.

Dataset 6: XRF_data

This dataset includes a table of the X-ray fluorescence data presented in [9] for TAS1402 reference composite depth LAN2 at 0.02 cm interval. Data includes the kilo counts per second (kcps), pass-through radiation (RAD) as a proxy for density, incoherence/coherence as a proxy for organic content, aluminum (Al), potassium (K), titanium (Ti), lead (Pb) and elemental ratios (Pb/Al, Ti/K).

2. Experimental Design, Materials and Methods

2.1. Core correlation

Correlation of the lake sediment cores is based on a series of 24 stratigraphic tie-points identified visually and one tie-point from the incoherence on coherence ratio (inc/coh) data. The later is a proxy for the organic content in the sediment that is obtained from micro-XRF core scanning. Correlating the gravity core (LA) and the Nesje cores (N1 and N2) was done using a large amplitude change in the inc/coh ratio (micro-XRF data) at 75 cm in LA, 29 cm in N1-A, and 25 cm in N2-A. The inc/coh tie-point depth is where the maximum inc/coh value is found after the inflection. The reference depth record used in this work is the composite depth LAN2. All data measured on samples from core N1 (OSL, beryllium, and magnetism) was transferred to the reference depth LAN2 using a linear interpolation transfer function using the 24 visual stratigraphic tie-points delimiting facies (see Sup. Mat. 2 of [9]). Thus, constant sedimentation rate is assumed within each individual facies. The section N2-A stratigraphy may be disturbed as a sediment gap formed at 114 cm depth LAN2 during core splitting operations with the two sections labelled N2-A-a and N2-A-b.

2.2. Micro-XRF core scanning

The split cores were scanned using Cox Analytical System's micro X-ray fluorescence Itrax core scanner at the Australian Nuclear Science and Technology Organisation (ANSTO). The elemental composition was measured and X-ray radiograph, pass-through radiation (RAD) and optical images were acquired. The element measurements were conducted at 0.02 cm interval with a molybdenum (Mo) target tube set at 30 kV and 55 mA. The RAD was measured at 0.05 cm interval. The RAD settings were adjusted to the density of the cores and corresponded to values of 50 kV to 55 kV and 30 mA. The analysis and data processing software was a Cox Analytical System by Q-Spec.

All cores were cleaned prior to scanning to remove surface contamination then placed on the sample stage. An optical image and surface topography was obtained initially, after which the core was covered using a Mylar film of 2 μm thickness. All parameters for analysis are set using a point analysis for 10 s. After this the model spectra are fitted for elements that are present at that spot. The pass through radiation scan is carried out first which is followed by the elemental scan. As it is a simultaneous technique, data is obtained at the same time for all elements. After the scan is complete, post-processing of data is carried out for all spectra using Q-Spec software. The data collected includes a document file with all the settings, an optical and RAD file, spectra files with all the spectra collected at each interval and a text file with all the elemental data. The elements included in this dataset are aluminium (Al), potassium (K), titanium (Ti), and lead (Pb). RAD is a density proxy and inc/coh is an organic content proxy.

2.3. Radiocarbon dating

The reference depth profile composed of the core sections LA, N2-A and N2-B were sampled for radiocarbon dating, with each sample being of 0.5 cm thickness. The radiocarbon sample positions and core photographs are provided in the Supplementary Material 1 of [9]. 29 bulk sediment samples were sent for analysis at DirectAMS Radiocarbon Dating Service laboratory. The radiocarbon age estimates were calibrated with the Southern Hemisphere calibration curve ShCal20 [10].

2.4. Optically stimulated luminescence (OSL) dating

Samples for OSL dating were collected from core sections N1-A, N1-B, N1-C, and N2-D. The sampling strategy included 23 OSL samples and 21 more sediment samples from above, below and between each OSL sample in order to obtain field moisture content and environmental dose rate measurements (DOS samples), including reconstruction of the gamma dose rate. The pale yellow and more clastic sediment facies, rather than the organic-rich black sediment facies, were targeted for OSL dating. Samples were collected from one half of a split core that was exposed to light, so the first 0.5 cm of the surface of the split core that was exposed to light was first removed, leaving an ~2.5 cm deep sediment section for sampling. Samples were 3–7 cm thick, depending on the thickness of the sediment unit; care was taken not to cross-cut units.

Routine optical dating procedures were used for preparing samples [11]. First, sieving of sediment samples was conducted for obtaining a range of sand-sized particles fractions. Particles of 90–125 μm in diameter were targeted for dating. Second, these sands were treated to remove carbonates and organic matter with HCl acid and H_2O_2 solution, respectively. Third, the quartz grains were separated from heavy minerals in the sample using a sodium polytungstate solution of density 2.70 g/cm³. They were separated from feldspar using a density of 2.62 g/cm³. Very few heavy minerals or feldspar grains were obtained, which may be because of the very small starting mass of the bulk sediment sample. Fourth, the quartz grains were etched using 40% HF acid for 45 min in order to 1) dissolve any remaining feldspar grains in the quartz separates, and 2) take off the alpha-irradiated layer on the surface of every sand particle. Finally, the HF-etched quartz grains were rinsed in HCl acid to remove any precipitated fluorides and sieved again.

Following this procedure, only very small amounts of sand-sized quartz grains were extracted from the samples. Due to limited sample material and the clear stratigraphic facies arguing against pervasive sediment mixing, we used multi-grain aliquot OSL measurements to determine the equivalent dose (D_e) for each sample. For every sample, 6 to 10 aliquots (3 mm in diameter, each containing ~300 grains) were measured. OSL measurements were made on an automated Risø TL-DA-20 luminescence reader equipped with blue light-emitting diodes (LEDs) (470 nm) and infrared LEDs for optical stimulation [12]. Electron Tubes Ltd 9235QA photomultiplier were used for detection of luminescence emissions through Hoya U-340 filters. A $^{90}\text{Sr}/^{90}\text{Y}$ beta source calibrated using a range of known gamma-irradiated quartz was used to irradiate inside the luminescence reader.

The multi-grain quartz measurements were conducted using the single-aliquot regenerative-dose (SAR) method [13,14]. The SAR method involves OSL signals measurements from the natural (burial) dose (L_n) as well as from a series of regenerative doses (L_x) adequately bracketing the D_e value. The D_e value is obtained experimentally by means of the calibrated $^{90}\text{Sr}/^{90}\text{Y}$ beta source as described above. The aliquots were submitted to heat treatment at 240 °C for 10 s before optical stimulation was conducted with blue LEDs at 125 °C for 40 s. Following each L_n and L_x , a fixed test dose of ~5.4 Gy with pre heat treatment at 240 °C for 5 s was given. These induced OSL signals (T_n and T_x) were used for correcting eventual sensitivity changes during the SAR procedure. In addition, a duplicate regenerative dose in the sequence was included to verify the adequacy of this sensitivity change correction. Furthermore, a 'zero regenerative dose' (0 Gy) measurement cycle was also included to monitor the extent of any 'recuperation' impelled by the preheat treatment. Possible contamination of the acid-etched quartz grains by other mineral inclusions was checked by applying the OSL IR depletion ratio test [15] to each grain at the termination of the SAR procedure. This was done using an infrared exposure at 50 °C for 40 s. Reasons for rejecting aliquots include: (1) Recycling ratio (the ratio of L_x/T_x values for the duplicate regenerative doses) being not consistent with unity at 2σ , and (2) OSL IR depletion ratio being more than 2σ less than unity. The values for L_n , L_x , T_n and T_x were approximated from the first 0.8 s of OSL decay, with the last 8 s background mean count value subtracted. Sensitivity-corrected dose response curves (DRCs) were obtained from the L_x and T_x OSL signals using a saturating exponential function. The D_e value was estimated by interpolation, by projecting the sensitivity-corrected natural OSL signal (L_n/T_n) to the fitted DRC.

A series of dose recovery tests were performed to select appropriate measurement parameters [9]. Twenty-one aliquots of sample OSL5 were measured using a given dose of ~80 Gy and employing seven distinct preheat combinations including 180/180, 260/160, 180/160, 200/200, 220/220, 240/220 and 240/240. Accurate measured/given dose ratios were obtained for the two following combinations: 240 °C for 10 s (PH-1) and 240 °C for 5 s (PH-2) (mean = 1.01 ± 0.07 ; N = 3) and 220 °C for 10 s (PH-1) and 220 °C for 5 s (PH-2) (mean = 1.00 ± 0.06 , N = 3).

Environmental dose rates correspond to the sum of the gamma, beta, and cosmic-ray dose rates external to the grains, plus addition to a small alpha dose rate internal to the quartz grains (0.03 ± 0.01 Gy/ka). Present-day radionuclide activities and dose rates are considered to have prevailed throughout the period of sediment sample burial. The current moisture content of each OSL and DOS sample was measured to correct the gamma, beta and cosmic-ray dose rates, because water is effective at attenuating ionising radiation [16]. The current measured moisture content was assumed to be representative of the entire burial history of the sample, and was used in calculation of all environmental dose rate parameters. A 20% relative error was applied to each estimate to accommodate the likely range of water contents experienced by these deposits during their burial history. Uranium, thorium and potassium concentrations data acquired from inductively coupled plasma mass spectrometry (ICP-MS) and optical emission spectroscopy (ICP-OES) were converted to gamma dose rates using the conversion factors of Aitken [11]. The gamma dose environment for each OSL sample was reconstructed using the proportional distribution of gamma rays within the 30 cm sphere around a sample, following the conceptual model of Aitken (1985). Beta dose rates were estimated from GM-25-5 beta counting using the procedures described and tested previously [12], including a correction for grain size [13]. The accuracy of the beta dose rates were verified by calculating the beta dose rates from the U, Th and K values obtained from ICP-MS(OES). The cosmic-ray dose rates were calculated following Murray and Wintle [14]. The cosmic-ray dose rates are adjusted for site altitude, geomagnetic latitude, density (sediment = 1.8 g/cm³; water = 1.025 g/cm³) and thickness of sediment overburden, and an average permanent water depth of 5 m. It was assumed that compaction and de-watering during core extraction has not had a major impact.

The weighted mean De calculated from the 6–10 multi-grain aliquots using the central age model of [13], divided by the environmental dose rate, which is the sum of the internal alpha and external beta, gamma and cosmic-ray dose rates, gives the burial time of the grains in calendar years ago. Age uncertainties are given at 1σ standard error on the mean. This was done by combining in quadrature all known and estimated sources of systematic and random errors.

2.5. Magnetic analysis

Standard paleomagnetic 8 cm³ (plastic box of dimension 2 × 2 × 2 cm) cube samples were taken contiguously from cores LA, N1-A, N1-B, N1-C, N2-C, and N2-D. In order to obtain duplicate measurements over the time of the Laschamp geomagnetic excursion, the core N2-A (24–81.6 cm section depth) was also sampled. In total, 287 cube samples and 24 discrete samples (~ 1 g) were analysed at the Australian National University (Australia). Magnetic analyses of the cube samples include (i) low field volumetric magnetic susceptibility (klf) at operating frequency 976 Hz measured with an AGICO Kappabridge model MFK1 and Safyr software, and (ii) the natural, anhysteretic, and isothermal remanent magnetizations (NRM, ARM, and IRM, respectively) measured with a 2G Enterprise cryogenic magnetometer model 755 and in-house software. The cryogenic magnetometer was used in a magnetically shielded room at the ANU Black Mountain Paleomagnetic Laboratory. First, the NRM was demagnetized with in-line alternating field (AF) in 13 steps to maximum alternating field (AF) of 90 mT. The software Puffinplot [1] was used to analyze the results with unanchored principal component analysis (PCA). The cores were not oriented azimuthally during coring. Thus, the declination data are aligned from one core section to the next by subtracting the average declination of the non-anomalous values from each section. The second measurement with the 2G cryogenic magnetometer was the ARM. ARM was induced with a direct current field of 0.05 mT and peak AF of 100 mT and demagnetized in 7

AF steps. The third measurement is the IRM. An IRM induced with 1 T field using a 2G pulse magnetizer was subsequently demagnetized in a series of 6 AF demagnetisation steps. Then a second IRM was induced with 0.3 T field in the opposite direction and measured with the 2G cryogenic magnetometer. The magnetic remanence data obtained from this suite of measurements was used to calculate coercivity indicators. These include i) the median destructive field (MDF), which is the field required to demagnetize half the initial remanence, ii) the ARM ratio (kARM/IRM), which is a proxy of the magnetic coercivity, (iii) the S-ratio (IRM-0.3T/IRM1T), which is a proxy for the relative contributions of low and high coercivity minerals to the total IRM and (iv) the HIRM ((IRM1T +IRM-0.3T)/2), which is the absolute contribution of high coercivity minerals to the total IRM.

The 24 discrete samples were air dried and gently crushed using an agate mortar and pestle. Magnetic analyses of the discrete samples were performed with a Princeton Measurements Corporation (now Lake Shore Cryotronics) Vibrating Sample Magnetometer (VSM) model 3900 to further characterise the magnetic mineral assemblage. The analyses include hysteresis loops with slope correction (direct moment vs. field settings: field range 1T, averaging time 150 ms), IRM acquisition up to 1T and back field curves (averaging time 200 ms). The magnetic properties obtained from these measurements on discrete samples were used to calculate proxies of magnetic grain size and mineralogy. These include the remanence ratio (saturation remanence (Mrs)/saturation magnetisation(Ms)) and the coercivity ratio (the remanent coercive force (Hcr)/bulk coercive force (Hc)) calculated from hysteresis loop and back field curve data. The software MAX UnMix [2] was used to analyse IRM acquisition curves. First-order reversal curves (FORC) were acquired on 4 samples and processed using FORCinel [3] with VARIFORC smoothing [4] parameters sc0=4-5, sc1=5-6, sb0=4, sb1=7-8, lambda=0.12 (Fig. 7 in [9]). Thermomagnetic curves (high-temperature and low temperature) were acquired for two representative samples N1-A18 (interglacial sediment) and N1-C37 (glacial sediment). High-temperature measurement of magnetic susceptibility from room temperature to 700 °C was done with a AGICO MFK2 Kapabridge and CS4 high temperature furnace apparatus controlled by the software Sufyte. Data processing was done with the software Cureval. Low-temperature measurement of saturation isothermal remanent magnetisation (RTSIRM 5T) from room-temperature to 10 Kelvin was done using a Quantum Design Magnetic Property Measurement System (MPMS).

2.6. Beryllium isotopes analysis

Samples for beryllium isotope analysis were collected from core sections N1-A and N1-B on one side of the trench left by paleomagnetic cube sampling. Care was taken to ensure the beryllium isotopes sampling depths correspond to the paleomagnetic sample depths. A total of 45 samples were analysed following the method established by Bourlès et al. [17] and revised by Simon et al. [18] at CEREGE National Cosmogenic Nuclides Laboratory (France). Authigenic ^{10}Be and its stable isotope ^{9}Be were extracted from ~ 1 g dry sample by soaking the samples in 20 ml of leaching solution at 95 ± 5 °C for 7 h. The leaching solution was composed of 0.04 M hydroxylamine ($\text{NH}_2\text{OH}-\text{HCl}$) and 25% acetic acid.

The resulting leaching solution was sampled with 2-ml aliquot for measurement of the natural ^{9}Be concentration with a graphite-furnace atomic absorption spectrophotometer (AAS) employing a double beam correction (Thermo Scientific ICE 3400). In order to eliminate matrix effects during the absorption and to allow measurements near the detection limit, a standard-addition method adding a constant volume of MgNO_3 solution were utilized. Four 100 ml aliquots of the sample solution were used for the determination of ^{9}Be sample concentrations using repeated absorbance measurements (4 times). Three of the aliquots were spiked with increasing amount of a Sharlau ^{9}Be -carrier diluted to a known concentration ($0.27\text{--}0.34 \times 10^8 \text{ g.g}^{-1}$) using HNO_3 0.2%. The standard deviation of these repeated absorbance measurements must be less than 3% for each sample to be accepted, and this constitutes a measurement quality control. The associated uncertainties (2σ) represent the reproducibility of measure-

ments calculated from the least-square fit between the measured absorbance at each stages of the standard-addition method ($r^2 > 0.9995$).

The remaining leaching solution was then spiked with 300 μl of a $9.8039 \times 10^{-4} \text{ g.g}^{-1}$ ^{10}Be -carrier and Be purification was performed in a two-stages column chromatography. In preparation for each separation stages, the samples were evaporated and dissolved in ultra-pure HCl and the Be oxy-hydroxides were precipitated at pH 8.5 by adding NH₃. The precipitate could then be separated by centrifugation, and subsequently dissolved in ultra-pure HCl for processing onto a column loaded with 15 ml of specific ion-exchange resins. Iron (Fe) and manganese (Mn) were separated using a Dowex® 1 × 8 (100 - 200 mesh) anion-exchange resin. The resin was rinsed with 20 ml MilliQ® water and conditioned with 20 ml 10.2 M HCl. The sample was then loaded onto the column and the Be fraction was collected immediately using 20 ml 10.2 M HCl for elution. The next purification step was to separate Boron (B) and Aluminum (Al) with a Dowex® 50 × 8 (100 - 200 mesh) cation-exchange resin. The resin was rinsed with 30 ml MilliQ® water and conditioned with 30 ml 1 M HCl. After loading the sample onto the column, the B and Be were successively eluted in 40 ml and then 120 ml of 1 M HCl while the Al remained trapped within the column. After completing these two separation stages, NH₃ is added to the solution to precipitate Be oxy-hydroxides at pH 8.5. The precipitate was then separated by centrifugation, rinsed by re-suspension using pH 8.5 buffered MilliQ® water and centrifuged a second time. The purified Be oxy-hydroxides were solubilized in HNO₃ and transferred into a quartz crucible for gentle evaporation at 200 °C until fully dry. Finally, the Be oxy-hydroxides dry deposit was oxidized into BeO by heating at 800 °C for 1 h. The BeO was then mixed with Nb powder and the mixture was pressed into a cleaned Ti cathode-holder for AMS measurements. Several routine blanks and 2 replicates were also measured in order to routinely assess cleanliness and reproducibility during the chemical extraction. Once the samples are ready, the accelerator mass spectrometer (AMS) measurements of $^{10}\text{Be}/^{9}\text{Be}$ ratios are performed. The ^{10}Be concentrations are calculated from the measured spiked $^{10}\text{Be}/^{9}\text{Be}$ ratios normalised to the BeO STD-11 in-house standard ($1.191 \pm 0.013 \times 10^{-11}$). Finally, the ^{10}Be half-life ($T_{1/2}$) of 1.387 ± 0.012 Ma and the dipole-independent age model are used to calculate the decay-corrected authigenic ^{10}Be concentrations.

Ethics Statement

None.

Declaration of Competing Interest

The authors declare that they have no known competing financial interests or personal relationships which have or could be perceived to have influenced the work reported in this article.

Data Availability

Chronostratigraphy of a 270-ka sediment record from Lake Selina, Tasmania: Combining radiometric, geomagnetic and climatic dating (Original data) (PANGAEA).

CRediT Author Statement

Agathe Lisé-Pronovost: Conceptualization, Methodology, Formal analysis, Investigation, Data curation, Writing – original draft, Funding acquisition; **Michael-Shawn Fletcher:** Conceptualization, Methodology, Resources, Writing – review & editing, Funding acquisition; **Quentin Simon:** Investigation, Resources, Writing – review & editing; **Zenobia Jacobs:** Investigation, Resources,

Writing – review & editing; **Patricia S. Gadd:** Investigation, Resources, Writing – review & editing; **Andy I.R. Herries:** Resources, Writing – review & editing; **Yusuke Yokoyama:** Methodology, Writing – review & editing.

Acknowledgments

Thanks to the TAS1402 drilling team (Kristen K. Beck, Alexa Benson, Angelica Ramirez, William Rapuc, Anthony Romano) and the data science support team (Milan Korbel, Shashwat Pathak, Lachlan Simpson). This research was supported by use of the Nectar Research Cloud; a collaborative Australian research platform supported by the National Collaborative Research Infrastructure Strategy (NCRIS). We thank Maarten Blaauw for support with rbacon and Xiang Zhao and Andrew Roberts for assistance at the Paleomagnetism Laboratory at the Australian National University. This project was funded by the Australian Research Council Discovery Indigenous IN140100050 to M.-S. Fletcher and IN170100062 to M.-S. Fletcher and A. Lise-Pronovost. A. Lise-Pronovost was supported by a La Trobe University DVCR Fellowship and a University of Melbourne McKenzie Fellowship. D. Heslop was supported by the [Australian Research Council \(DP190100874\)](#). The ASTER AMS national facility (CEREGE, Aix en Provence) is supported by INSU/CNRS, ANR through the EQUIPEX “ASTER-CEREGE” action, and IRD.

References

- [1] P.C. Lurcock, G.S. Wilson, PuffinPlot: a versatile, user-friendly program for paleomagnetic analysis, *Geochem. Geophys. Geosyst. G-cubed* 13 (2012) Q06245, doi:[10.1029/2012GC004098](https://doi.org/10.1029/2012GC004098).
- [2] D.P. Maxbauer, J.M. Feinberg, D.L. Fox, MAX UnMix: a web application for unmixing magnetic coercivity distributions, *Comput. Geosci.* 95 (2016) 140–145, doi:[10.1016/j.cageo.2016.07.009](https://doi.org/10.1016/j.cageo.2016.07.009).
- [3] R.J. Harrison, J.M. Feinberg, FORCinel: an improved algorithm for calculating first-order reversal curve distributions using locally weighted regression smoothing, *Geochem. Geophys. Geosyst. G-cubed* 9 (2008) Q05016, doi:[10.1029/2008GC001987](https://doi.org/10.1029/2008GC001987).
- [4] R. Egli, VARIFORC: an optimized protocol for calculating non-linear first-order reversal curves (FORC) diagrams, *Glob. Planet. Chang.* 110 (2013) 302–320, doi:[10.1016/j.gloplacha.2013.08.003](https://doi.org/10.1016/j.gloplacha.2013.08.003).
- [5] L. Bøtter-Jensen, C.E. Andersen, G.A.T. Duller, A.S. Murray, Developments in radiation, stimulation and observation facilities in luminescence measurements, *Radiat. Meas.* 37 (2003) 535–541.
- [6] L. Bøtter-Jensen, V. Mejdhahl, Assessment of beta-dose-rate using a GM multicontainer system, *Nucl. Tracks Radiat. Meas.* 14 (1988) 187–191.
- [7] Duller, G.A.T., 2018. Analyst v4.57. User manual. users.aber.ac.uk/ggd/analyst_manual_v4_57.pdf.
- [8] A. Nesje, A piston corer for lacustrine and marine sediments, *Arct. Alp. Res.* 24 (1992) 257–259, doi:[10.1080/00040851.1992.12002956](https://doi.org/10.1080/00040851.1992.12002956).
- [9] A. Lise-Pronovost, M.S. Fletcher, Q. Simon, Z. Jacob, P. Gadd, D. Heslop, A.I.R. Herries, Y. Yokoyama, Chronostratigraphy of a 270-ka sediment record from Lake Selina, Tasmania: combining radiometric, geomagnetic, and climatic dating, *Quat. Geochronol.* 62 (2021) 101152, doi:[10.1016/j.quageo.2021.101152](https://doi.org/10.1016/j.quageo.2021.101152).
- [10] A. Hogg, T. Heaton, Q. Hua, J. Palmer, C. Turney, J. Southon, A. Bayliss, P. Blackwell, G. Boswijk, C. Bronk Ramsey, F. Petchey, P. Reimer, R. Reimer, L. Wacker, SHCal20 Southern Hemisphere calibration, 0–55,000 years cal BP, *Radio-carbon* 62 (2020), doi:[10.1017/RDC.2020.59](https://doi.org/10.1017/RDC.2020.59).
- [11] M.J. Aitken, *An Introduction to Optical Dating*, Oxford University Press, Oxford, 1998.
- [12] L. Bøtter-Jensen, C.E. Andersen, G.A.T. Duller, A.S. Murray, Developments in radiation, stimulation and observation facilities in luminescence measurements, *Radiat. Meas.* 37 (2003) 535–541.
- [13] R.F. Galbraith, R.G. Roberts, G.M. Laslett, H. Yoshida, J.M. Olley, Optical dating of single and multiple grains of quartz from Jinmium rock shelter, northern Australia: Part I, experimental design and statistical models, *Archaeometry* 41 (1999) 339–364, doi:[10.1111/j.1475-4754.1999.tb00987.x](https://doi.org/10.1111/j.1475-4754.1999.tb00987.x).
- [14] A.S. Murray, A.G. Wintle, Luminescence dating of quartz using an improved single-aliquot regenerative-dose protocol, *Radiat. Meas.* 32 (2000) 57–73.
- [15] G.A.T. Duller, Distinguishing quartz and feldspar in single grain luminescence measurements, *Radiat. Meas.* 37 (2003) 161–165.
- [16] R.P. Nathan, B. Mauz, On the dose-rate estimate of carbonate-rich sediments for trapped charge dating, *Radiat. Meas.* 43 (2008) 14–25.
- [17] D.L. Bourlès, G.M. Raisbeck, F. Yiou, ¹⁰Be and ⁹Be in Marine sediments and their potential for dating, *Geochim. Cosmochim. Acta* 53 (2) (1989) 443–452, doi:[10.1016/0016-7037\(89\)90395-5](https://doi.org/10.1016/0016-7037(89)90395-5).
- [18] Q. Simon, N. Thouvenot, D.L. Bourlès, L. Nuttin, G. St-Onge, C. Hillaire-Marcel, Authigenic ¹⁰Be/⁹Be ratios and ¹⁰Be-fluxes (230Thxs-normalized) in central Baffin Bay during the last glacial cycle: paleoenvironmental implications, *Quat. Sci. Rev.* 140 (2016) 142–162, doi:[10.1016/j.quascirev.2016.03.027](https://doi.org/10.1016/j.quascirev.2016.03.027).